Electrical Power and Energy Systems 136 (2022) 107764

Contents lists available at ScienceDirect

International Journal of Electrical Power and Energy Systems

journal homepage: www.elsevier.com/locate/ijepes

An optimized multi-objective reactive power dispatch strategy based on improved genetic algorithm for wind power integrated systems

Yichen Liu [a], Dragan Ćetenović [a,c], Haiyu Li [a,*], Elena Gryazina [b], Vladimir Terzija [b]

[a] Department of Electrical and Electronic Engineering, University of Manchester, Sackville Street, Manchester M13 9PL, UK
[b] Center for Energy Science and Technology (CEST), Skolkovo Institute of Science and Technology, Bolshoy Boulevard 30, Bld. 1, Moscow 121205, Russia
[c] University of Kragujevac, Faculty of Technical Sciences Čačak, Svetog Save 65, 32000 Čačak, Serbia

ARTICLE INFO

Keywords:
Forecast error
Genetic algorithm
OLTC
Reactive power optimization
Voltage control
Wind turbines

ABSTRACT

The large uncertainties in wind power generation will bring great challenges to the analysis of optimal reactive power dispatch (ORPD). This paper considers a multi-objective ORPD strategy solved by a heuristic search algorithm that combines the elitist non-dominated sorting genetic algorithm with inheritance (i-NSGA-II) and a roulette wheel selection to optimize the operation of wind power integrated systems. The proposed ORPD strategy employs day-ahead predicted wind energy and load demand data to optimally set of the following control variables: i) optimal tap positions of on-load tap changers (OLTCs), ii) reactive demand set point of reactive power compensators and iii) active and reactive power outputs of wind farms (WFs) with the objectives to minimize: a) voltage deviations, b) active power loss, c) wind turbine harmonic distortions and d) number of switching operations of OLTCs. Because of the uncertainties of wind energy and load demand, hourly modifications of the day-ahead optimal results are also formulated to determine the real-time optimal reactive power dispatch. The proposed new ORPD strategy has been rigorously tested using IEEE 33-bus test system, PG&E 69-bus test system and modified real GB network. Results obtained confirmed the efficacy and applicability of the proposed strategy in both distribution and transmission networks.

1. Introduction

Recently, as a result of large-scale wind farm integration in both transmission and distribution networks, significantly increased risks of voltage fluctuation and cascading tripping in transmission networks, as well as much higher voltage rise and drop fluctuation leading to poor power quality in distribution networks, have been reviewed and reported [1]. Facing emerging these challenges, authors suggests that current voltage control methods may not be sufficient to just maintain acceptable voltage profiles, so that a proper optimization strategy in both transmission and distribution systems is needed. To operate power systems in a secure, economic and stable manner with large-scale wind farm integration, optimized reactive power dispatch (ORPD) is one of the key measures to mitigate the risks of voltage fluctuations [2–4].

Existing ORPD strategies normally optimize single or two objectives, such as power loss and voltage deviations. This is solved by adjusting the generators VAr outputs, transformer taps and capacitors/reactors or reactive compensators with well-established objective functions under various constraints (such as network configurations). In addition, impact of more often OLTCs switching operations and increasing harmonic emissions from wind farms on network operation assets life have been reported in [5] and [6], respectively. Consequently, minimizing the number of switching operations of OLTCs has been considered in the various studies [7,8], and harmonic emission regulation for wind farms has been included in the relevant network operator codes [9]. This creates a need to include both switching operation times of OLTCs and harmonic emission as two additional objectives for ORPD strategy in wind power integrated systems.

Principally, ORPD can be formulated as a mixed integer, multi-variable, multi-constraints, non-linear, non-convex problem. To solve an objective function of ORPD problem, various strategies based on classical methods have been proposed in [8,10–18]. By considering an ORPD problem as a second-order cone (SOC) programming problem, distributionally robust optimization with wasserstein distance is used to address the uncertainties for ORPD in active distribution networks [10]. By using branch flow model-based relaxed power flow, a coordinated

* Corresponding author.
E-mail addresses: yichen.liu@postgrad.manchester.ac.uk (Y. Liu), dragan.cetenovic@manchester.ac.uk (D. Ćetenović), haiyu.li@manchester.ac.uk (H. Li), e.gryazina@skoltech.ru (E. Gryazina), v.terzija@skoltech.ru (V. Terzija).

https://doi.org/10.1016/j.ijepes.2021.107764
Received 4 October 2021; Accepted 27 October 2021
Available online 16 November 2021
0142-0615/

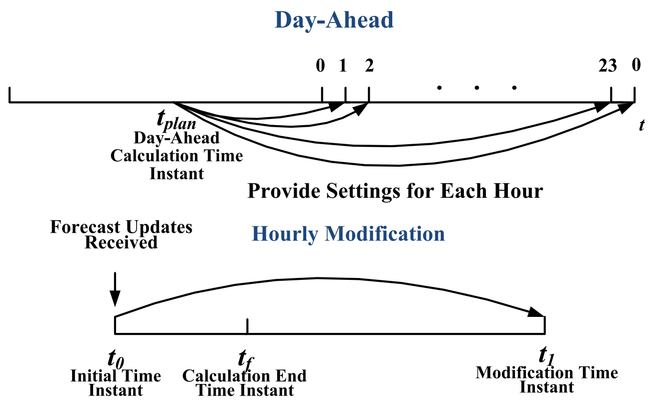

Fig. 1. Time scale of the ORPD strategy for wind power integrated power system.

optimization problem for active and reactive power dispatch as a mixed integer SOC programming problem has been solved in [11]. To address the uncertainties of various components in active distribution networks, such as distributed generations, two-stage classical optimization models are reviewed [12–17]. In [12], a mixed integer convex programming model is used. In [13], a risk-based mixed integer quadratically-constrained model for the long-term VAr planning problem with multiple objectives has been proposed. In [14], data-driven stochastic programming model is proposed and formulated as a two-stage problem. Similar strategy is also used in [15] to address the energy and reserve dispatch problem in renewable energy integrated systems to minimize system generation costs. Furthermore, a two-stage algorithm based long-term reactive power sources placing is proposed for large transmission networks in [16]. A pseudo-decoupling dispatch strategy based two-stage robust optimization has been proposed in [17] to minimize network loss in distribution network. The nonlinearity of ORPD equations is handled by a successive linear approximation approach in [8] in transmission networks. A simplified convex problem is obtained by linearizing the constraints [18], in which it characterizes the dispatch approximation errors between the original non-convex economic dispatch problem and the solutions of commonly used approximated convex relaxation classical methods. Nevertheless, this type of approximation approach show large error in the application to realistic transmission systems. According to literature [19], algorithmic recommendations for different types of networks, for radial distribution networks, the approximation error can still be neglected by solving an optimization problem based on branch flow model (BFM). However, for mesh networks, especially large networks with higher level complexity, a heuristic search algorithm can be worth exploring for finding feasible solutions within limited time.

With the advance of artificial intelligence algorithms and considerable increasing in the computational power, various heuristic search algorithms, such as differential evolution algorithm [20], cuckoo search algorithm [21], jellyfish search algorithm [22], and salp swarm algorithm [23] have been considered to solve ORPD problems. However, for a complex multi-objective optimization problem, they may easily lead to local optimal solutions due to non-convexity of the ORPD problem and different directional or conflicting objectives of the objective functions [3]. To address multiple objective optimizing problem challenges, various methods, such as an improved heap-based optimizer [24], teaching learning based optimization [25], firefly algorithm [26], oppositional krill herd algorithm [27], particle swarm optimization [28], artificial bee colony [29], genetic algorithm considering dynamic crowding distance [30] or genetic algorithm incorporating fuzzy for both radial network reconfigurations and losses [31], multi-objective evolutionary algorithm [32] and adaptive immune algorithm [33] have been proposed and considered to solve multi-objective ORPD problem.

So far most ORPD strategies are designed for distribution networks considering only single or two objectives such as power losses and voltage deviations. For large wind farm integration systems with significant voltage variation, it may be also necessary to consider reducing both OLTC switching operations and harmonic emissions. Moreover, there is a need to include the consideration of large wind generation and load demand variations hourly. These additional considerations with a larger number of control variables would make the objective function solving process for ORPD problem more complex. Hence, more efficient and faster optimal computational algorithm would be necessary. In this paper, to apply the proposed strategy in both distribution and transmission networks and to avoid approximation error, a heuristic search algorithm is used. Therefore, we consider a multi-objective OPRD strategy solved by a heuristic search algorithm that combines the elitist non-dominated sorting genetic algorithm with inheritance (i-NSGA-II) [34] and a roulette wheel selection [35]. Using this algorithm, fast convergence keeping the same level of accuracy has been achieved in order to optimize the operation of power system with integrated wind farms. By formulating hourly modifications of the day-ahead optimal results based on critical real-time measurements, this paper will show a significant improvement for determining both the day-ahead and real-time ORPD application in wind power integrated systems. By solving the proposed objective function using applied improved genetic algorithm, the solving process is more computationally efficient compared with other heuristic search algorithms.

Main contributions of this paper are as follows:

i) a new strategy with a more complex objective function for solving ORPD problem is proposed, considering simultaneously power losses, voltage deviations, operation times of OLTCs and wind turbine harmonics emission;
ii) more control devices are considered which means optimal engagement of wind turbines, reactive power compensators and transformers equipped with OLTCs are well-thought-out;
iii) an improved algorithm, that combines two major GA based adjustments together, solves the formulated multi-objective optimization problem faster so the proposed strategy can be applied into both day-ahead and hourly modifications;
iv) the proposed ORPD strategy are applied in both distribution and transmission networks.

In this paper, two distribution systems, IEEE 33 bus and PG&E 69 bus systems and one transmission system, a modified real GB network and its real data are used for simulation of day-ahead and hourly optimizations to prove that the proposed ORPD strategy can calculate the optimal solution by improved GA for both distribution and transmission systems and can be achieved within reasonable calculation time. All simulations have been done in MATLAB.

2. Optimized reactive power dispatch strategy in power systems with integrated wind turbines

In this Section, a new ORPD strategy including (i) a day-ahead planning based on forecast data and (ii) hourly modifications based on real-time measurement, is presented with multi-objective function, system constraints and control variables defined, as well as an improved GA for finding optimal solution for the created multi-objective optimization problem. In Fig. 1, time scales for implementing the proposed ORPD strategy in both day-ahead and hourly time are given. Note that the hourly modifications are triggered only when the differences between forecast inputs of day-ahead optimization and real-time measurement are above a threshold value which means a forecast updates received. If not, the modifications for that particular hour should not be performed and the day-ahead outputs should be used.

Firstly, the proposed strategy assumes a day-ahead planning, undertaken at the moment t_{plan}. In this time scale, *control variables*, i.e.

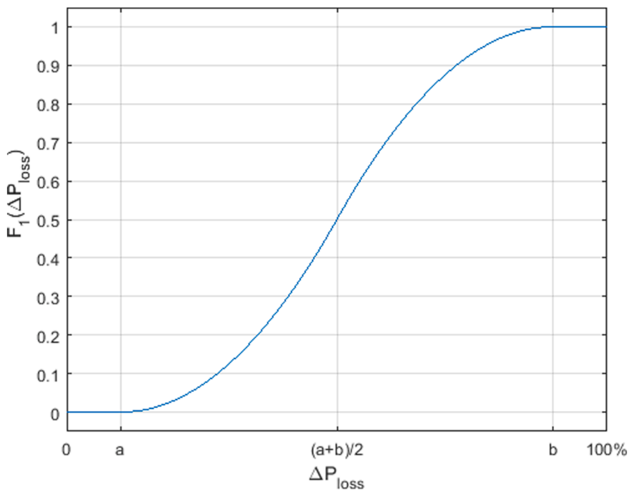

Fig. 2. S-type membership function.

active and reactive output power for WTs, injected reactive power for shunt capacitors (SCs), Static VAr Compensators (SVCs) and tap positions for OLTCs, are determined for each hour. They are used as initial settings for the hourly modifications at t_0, in which the inputs were updated using hourly real-time data, which are considered to be more reliable and less uncertain compared to the forecasted inputs used for the day-ahead time. Both day-ahead and hourly optimal solutions are obtained using an improved GA described later in this Section. The new ORPD strategy is described in Subsections below.

2.1. Day-ahead optimization

The role of the day-ahead ORPD is to optimally operate the system and consequently to ensure sufficient safety margins. The proposed multi-objective constrained optimization strategy considers a) tap positions of OLTCs, b) capacitances of SCs and SVCs, and c) active and reactive powers of WTs. They are belonging to the set of control variables, dominating in the day-ahead optimization of the ORPD strategy. The optimization is based on the following four criteria:

(i) to minimize the network active power losses, ΔP_{loss},
(ii) to minimize voltage deviations across the network, ΔU_{ave},
(iii) to minimize the number of tap switching operations caused by tap staggers and
iv) to minimize the system average total harmonic distortion (*SATHD*).

These above-mentioned criteria may have different levels of importance depending on the system planning and operation priorities. Criteria priorities are modelled by introducing adequate, prescribed weighting factors ω_1, ω_2, ω_3 and ω_4, respectively. Therefore, a day-ahead multi-objective optimization function can be formulated as follows:

$$minF = \omega_1 F_1(\Delta P_{loss}) + \omega_2 F_2(\Delta U_{ave}) + \omega_3 N_{TAP} + \omega_4 SATHD \tag{1}$$

where $F_1(\Delta P_{loss})$ and $F_2(\Delta U_{ave})$ are satisfaction functions related to active power losses and average system voltage deviation, N_{TAP} is the total tap step difference from initial tap positions for all OLTCs existing in the system and *SATHD* is the system average THD. The first two objective functions are traditionally considered as the most important criteria. Keeping them just within predefined limits would not lead to minimal losses and smallest voltage deviations. That is why for both mentioned criteria, adequate satisfaction functions have to be selected, what is described below.

Firstly, the power losses are calculated as follows:

$$\Delta P_{loss} = \sum P^{grid} + \sum P^{WT} - \sum P^{loads} \tag{2}$$

where *S*-type membership function is used [29]:

$$F_1(\Delta P_{loss}) = \begin{cases} 0 \quad \text{if } \Delta P_{loss} \leqslant a \\ 2\left(\dfrac{\Delta P_{loss} - a}{b - a}\right)^2 \quad \text{if } a \leqslant \Delta P_{loss} \leqslant \dfrac{a+b}{2} \\ 1 - 2\left(\dfrac{\Delta P_{loss} - b}{b - a}\right)^2 \quad \text{if } \dfrac{a+b}{2} \leqslant \Delta P_{loss} \leqslant b \\ 1 \quad \text{if } \Delta P_{loss} \geqslant b \end{cases} \tag{3}$$

where P^{grid} , P^{WT} and P^{load} are active powers of the traditional generators, WTs and load respectively; a and b are pre- calculated minimum and maximum power losses. The minimum power losses, a, are calculated by running power flow assuming when all reactive power demand is compensated locally and all transmission lines only transfer active power. The maximum power losses, b, is the maximum allowable system power losses, which is calculated by running power flow assuming that Q is produced from synchronous generators only [29]. S-type membership function is shown in Fig. 2.

For the second criterion, the Gauss-type function is used [29]:

$$\Delta U_{ave} = \frac{\sum_{i=1}^{M} |U_i - U_{i\_nom}|}{M} \tag{4}$$

$$F_2(\Delta U_{ave}) = e^{(\Delta U_{ave} - c)^2/\sigma^2} \tag{5}$$

where U_{i_nom} is the nominal voltage at bus i of the M bus system, c and σ are the mean value and standard deviation of the voltage deviation set as 0 and 0.0425 pu, respectively.

For the third criterion, the total tap step difference is calculated as [7]:

$$N_{TAP} = \sum_{l=1}^{N} x_l \tag{6}$$

where x_l is the tap step difference from initial tap positions on OLTC at bus l and N is the total number of OLTCs in system.

The level of distortion of signals in the grid is considered in the fourth criterion, in which *SATHD* is the system average THD, calculated as follows [36,37]:

$$SATHD = \frac{\sum_{k=1}^{M} S_k THD_k}{S_{total}} \tag{7}$$

where S_k is the generated or consumed apparent power at bus k, THD_k is the total harmonic distortion at bus k and S_{total} is the total apparent power generated by the system. The information about the total harmonic distortion at each bus (THD_k) can be obtained using power quality meters, or other sensors capable of monitoring signal distortions. These data can be detected with built-in harmonic ratio function of sensors or watt meters [38].

The range of feasible values of all four criteria is different, requiring a shift to their *per unit* consideration. This challenge can be resolved by defining all four weighting factors as follows:

$$\begin{cases} \omega_1 = \mu_1 / F_{1\_max}, 0 \leqslant \mu_1 \leqslant 1 \\ \omega_2 = \mu_2 / F_{2\_max}, 0 \leqslant \mu_2 \leqslant 1 \\ \omega_3 = \mu_3 / N_{TAP\_max}, 0 \leqslant \mu_3 \leqslant 1 \\ \omega_4 = \mu_4 / SATHD_{\_max}, 0 \leqslant \mu_4 \leqslant 1 \end{cases} \tag{8}$$

where μ_1, μ_2, μ_3 and μ_4 are weighting coefficients representing the importance of each criterion in *per unit*, F_{1_max}, F_{2_max}, N_{TAP_max} and $SATHD_{\_max}$ are pre-calculated maximum values of each criterion. The weighting coefficients must meet the following condition:

$$\mu_1 + \mu_2 + \mu_3 + \mu_4 = 1 \tag{9}$$

The values of weighting coefficients have been set through a sensitivity study in this paper, as described in Section III. In real systems, it can be selected based on different system operation priority by independent system operators.

Based on (2) – (9), the results of the day-ahead optimization are optimal values for all *control variables*, i.e. a) tap positions of OLTCs, b) capacitances of SCs and SVCs, and c) active and reactive powers of WTs.

2.2. Hourly modifications

The day-ahead optimization is based on forecasted inputs, which can be significantly different than the actual inputs measured at the beginning of each hour of the day. To cope with this fact and to use more reliable real-time inputs, which as such would lead to optimal solutions valid for each new hour, an hourly modification can be introduced. This could cause excessive number of changes of the tap positions of the OLTCs, what would have impact on reducing of equipment life. That is why the hourly modification considers their positions delivered by the day-ahead optimization as unchanged, leading to the conclusion that $\omega_3 = 0$. Consequently, the hourly modification multi-objective function becomes:

$$minF = \omega_1 F_1(\Delta P_{loss}) + \omega_2 F_2(\Delta U_{ave}) + \omega_4 SATHD \tag{10}$$

Obviously, now there are only 3 criteria and consequently only 3 weighting factors which have the same nature as the weighting factors from the day-ahead optimization (equation (1)). However, they have different values, considering that:

$$\mu_1 + \mu_2 + \mu_4 = 1 \tag{11}$$

That is why, in general terms, these weighting coefficients have different values compared to those in day-ahead optimizations.

2.3. Constraints

All control variables and criteria should meet power flow constraints:

$$\begin{cases} P_i = U_i \sum_{j=1}^{M} U_j (G_{ij} cos\delta_{ij} + B_{ij} sin\delta_{ij}) \\ Q_i = U_i \sum_{j=1}^{M} U_j (G_{ij} sin\delta_{ij} - B_{ij} cos\delta_{ij}) \end{cases} \tag{12}$$

where G_{ij} and B_{ij} are admittance matrix's real and imaginary part and δ_{ij} is voltage angle difference between buses i and j. Also, the following technical constraints must be satisfied:

$$\Delta P_{loss\_min} \leqslant \Delta P_{loss} \leqslant \Delta P_{loss\_max} \tag{13}$$

$$U_{i\_min} \leqslant U_i \leqslant U_{i\_max} \tag{14}$$

$$TAP_{l\_min} \leqslant TAP_l \leqslant TAP_{l\_max} \tag{15}$$

$$SATHD \leqslant SATHD_{\_max} \tag{16}$$

where ΔP_{loss_min} and ΔP_{loss_max} are the minimum and maximum system power losses, U_{i_min} and U_{i_max} are minimum and maximum permissible voltages at bus i, TAP_{l_min} and TAP_{l_max} are the minimum and maximum limits for tap position of the OLTC at bus l and $SATHD_{\_max}$ is the permissible system average THD.

In the day-ahead ORPD strategy there exists additional constraint which is maximum number of operation times, O_{l_max}, the tap position can be changed per day:

$$0 \leqslant O_l \leqslant O_{l\_max} \text{ for } l = 1, ..., N \tag{17}$$

There is one more constraint, related to reactive power outputs of WTs, here Type 3, i.e. DFIG. According to [39–41], the following two reactive power limits have to be considered:

$$Q_{t,max}^{WT} = P_{t,max}^{WT} \sqrt{1/pf^2 - 1} \tag{18}$$

$$Q_{t,max}^{WT} = \sqrt{\left(S_{t,max}^{WT}\right)^2 - \left(P_{t,max}^{WT}\right)^2} \tag{19}$$

where $Q_{t,max}^{WT}$ is the reactive power limit of WT, $P_{t,max}^{WT}$ is the output active power limit of WT, pf is the power factor (in this paper $pf = 0.95$) and $S_{t,max}^{WT}$ is the apparent power limit of WT. To distinct these two options, (18) is considered as *Q-control strategy 1* and (19) as *Q-control strategy 2*.

With all above constraints ((12)-(19)) and the multi-objective function defined, the ORPD becomes a constrained multi-objective optimization problem, which can be solved using different solvers. An improved GA is proposed for solving the formulated problem. Its description is given in next Subsection.

2.4. Improved genetic algorithm

Genetic algorithm is an artificial intelligence algorithm for solving complex non-convex problems by simulating natural evolution process. For single-objective problems, GA shows its superiority. However, in the multi-objective optimization problem, the biggest problem is how to determine the fitness of each individual. Multi-objective optimization also known as Pareto optimization involves multi-objective functions. The NSGA-II algorithm was proposed by [42] on the basis of GA which is ideal for constrained multi-objective optimization problems like power system optimization. Furthermore, it has been significantly improved and made more computationally efficient by involving parent inheritance in [34]. To further improve the GA speed, when making selections, the roulette selection algorithm [35] is applied. These two adjustments contributed to the efficacy of the entire optimization, what is particularly important in a real-time application, in which a large number of variables have to be simultaneously processed.

In this Subsection the improved GA is described, whereas the new solver was tested in the next Section. When applying this improved genetic algorithm, a number of so-called *individuals* have to be defined. In this paper, each individual refers to a combination of control variables. Individuals are firstly randomly selected from predefined feasible space, determined by the constraints adopted for all control variables. They are then processed by selection, crossover, and mutation procedures.

In selection procedure, a roulette selection algorithm is used. Individuals in each new generation are eliminated like a slot on the roulette wheel. The probabilities of these individuals to be selected are equal to the probabilities of the stop point dropping into the slot when spinning the roulette wheel. For each individual, its slot size is decided according to the objective function result for this individual, which is calculated as:

$$P_m = F(m) / \sum_{m=1}^{N_P} F(m) \tag{20}$$

where P_m is the area size of a certain individual m on roulette which is also the selection probability of m, $F(m)$ is the multi-objective function adaptive value of m and N_P is the size of each population. Furthermore, individuals with best performance of each single criterion are also calculated in each generation. They also have a chance to generate children population using the *non-dominated elitist approach with inheritance*, even though they might not be the best result for the whole multi-objective function. However, they also have the possibility to generate the global optimal children population when having crossover. Additionally, for the first generation, inherently selected parents develop a better pool of parent chromosomes, called inheritance. This adjustment will produce a better pool of the child's chromosomes. After that the crossover procedure generates children according to probability of crossover. And then remaining children are generated by the mutation according to probability of mutation.

By including the above mentioned adjustments in selection

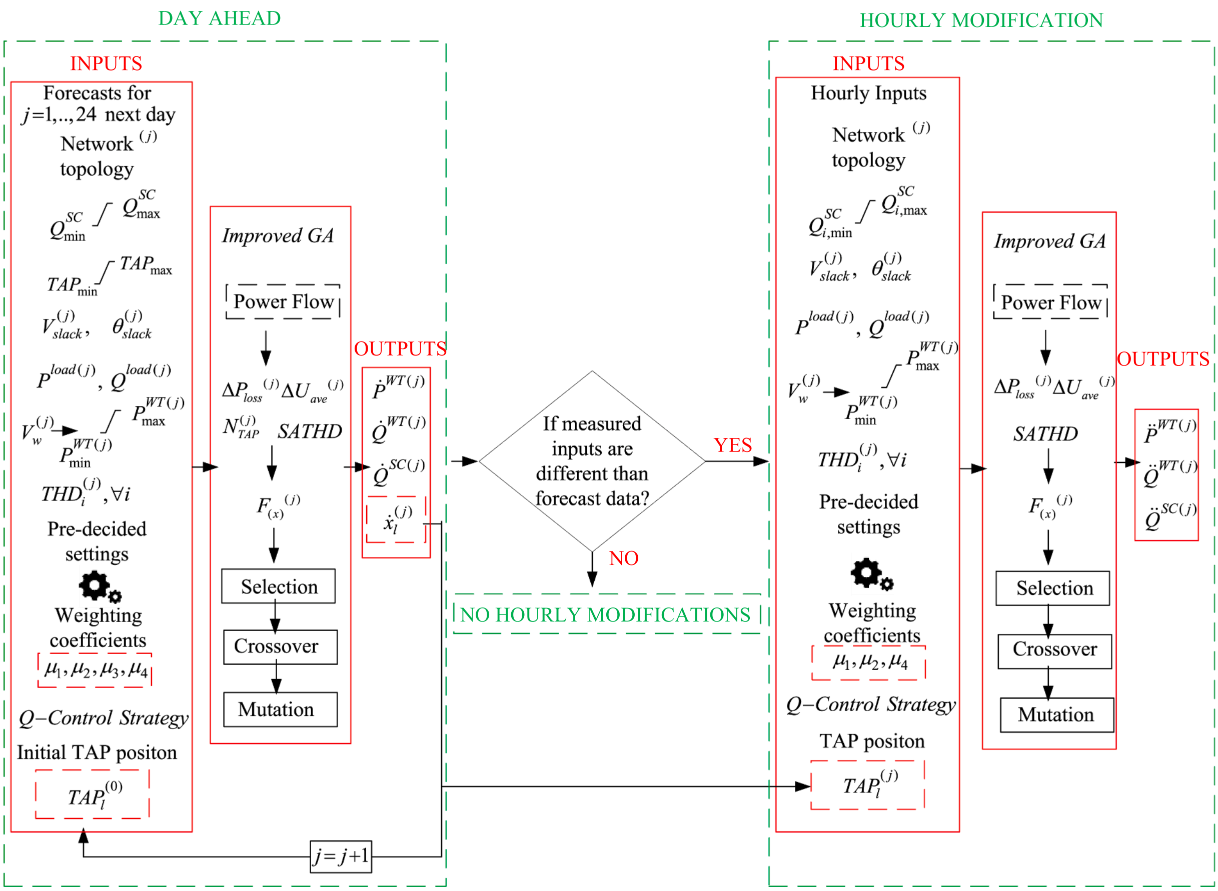

Fig. 3. Block diagram of the proposed ORPD strategy.

Table 1
Weighting coefficients setting scenarios.

	Day-ahead				Hourly Modification		
Scenario	μ_1	μ_2	μ_3	μ_4	μ_1	μ_2	μ_4
Setting 1	0.4	0.3	0.2	0.1	0.5	0.3	0.2
Setting 2	0.4	0.4	0.1	0.1	0.5	0.4	0.1
Setting 3	0.4	0.4	0.2	0	0.5	0.5	0

procedure, essentially smaller number of generations with a minimum number of function evaluations converging to the global optimal result is required. As it will be demonstrated in next Section by using conventional NSGA-II, some 100 generations are needed to reach the optimal solutions. On the other hand, improved GA converges to the optimal solution within 15 generations only, providing practically the same level of accuracy.

In this solver, to ensure that each selected individual has only the control variables within system constraints, the power flow calculation is included into the improved GA cycle. This will make the out-of-limit individuals to be sifted out immediately and consequently to achieve a better result for the objective function.

2.5. ORPD strategy block diagram

In Fig. 3, the entire ORPD strategy is depicted in a form of a block diagram. Here, V_{slack} and θ_{slack} are voltage magnitude and angle for selected slack bus, V_w is the wind speed, $\dot{Q}^{SC}$, $\dot{P}^{WT}$, $\dot{Q}^{WT}$, $\dot{x}_l$ are settings for control variables obtained as outputs from the day-ahead optimization and $\ddot{Q}^{SC}$, $\ddot{P}^{WT}$, $\ddot{Q}^{WT}$ are settings for control variables obtained as outputs from the hourly modifications. Note that the inputs for the day-ahead optimization are less reliable, since they are based on forecasted variables. Also note that in the hourly modifications, the OLTC criterion is not considered. The strategy has a routine, checking if the inputs for two optimizations are different. If they are, the hourly modifications should be performed. If they are not, the modifications for that particular hour should not be performed and the day-ahead outputs should be used. Based on a number of tests, a difference of more than 5 % indicates that the hourly modifications have to be performed.

The new strategy is tested using networks of different complexity and nature. Results are given in Section 3.

3. Testing of the new ORPD strategy

To test the proposed ORPD strategy, two distribution systems (IEEE 33-bus and PG&E 69-bus systems) and one transmission system (modified GB network) are used. Each test system has been extended with OLTCs (with switchable range from 0.9 to 1.1) and WTs (penetration level around 30%). Reactive power compensation existed in all test systems. When applying the improved GA, the crossover and mutation probability were respectively 0.8 and 0.3 [31,43]. It is also assumed that differences between inputs for both day-ahead and hourly optimizations obey Normal distribution [44,45].

3.1. Weighting coefficients settings

The entire testing required appropriate selection of weighting coefficients, so that three groups of *settings* are defined (see Table 1). Here *setting 1* is used for testing the strategy on all test systems, while *settings 2* and *3* are used for testing the strategy on PG&E 69-bus system.

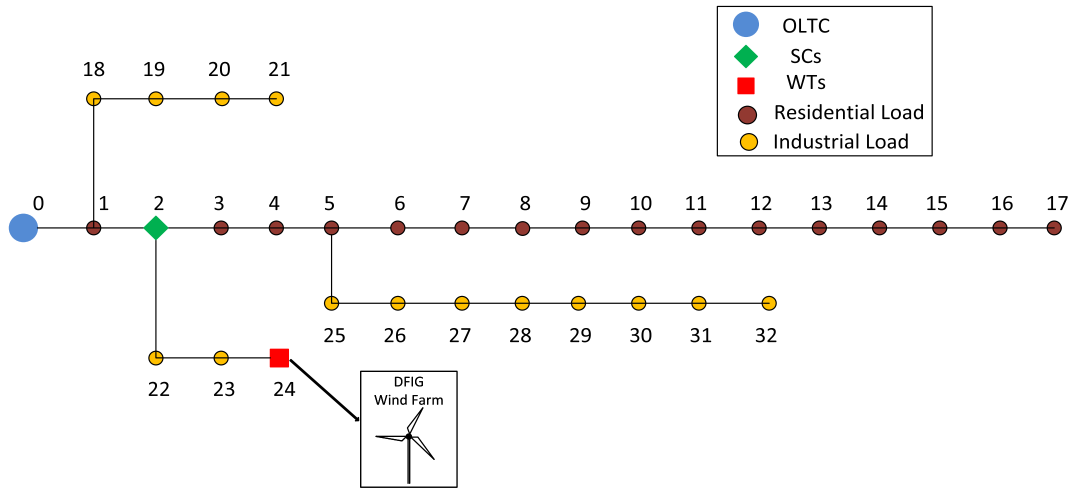

Fig. 4. Single line diagram of the modified IEEE 33-bus distribution system.

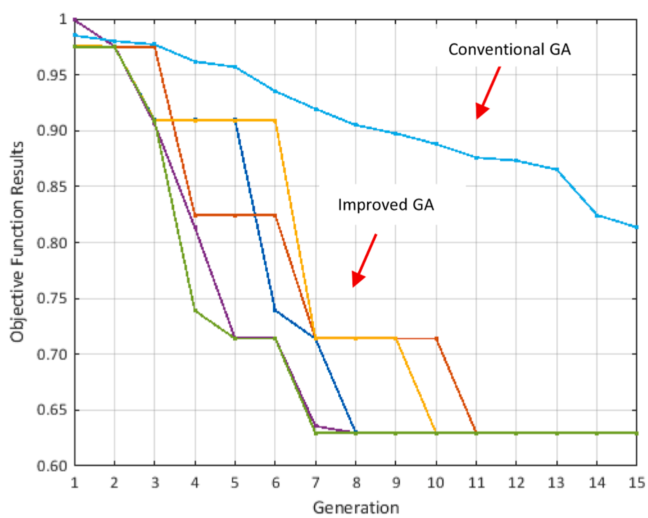

Fig. 5. Adaptive convergence characteristic curves.

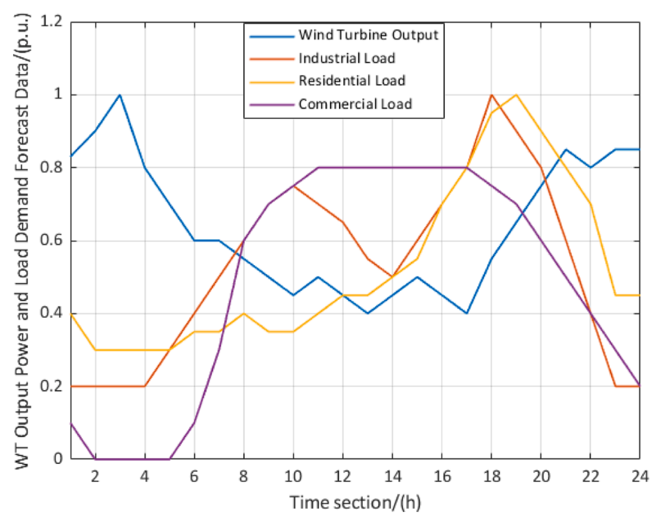

Fig. 6. Typical load demand and WT active power prediction curves [45].

Table 2
Comparison between Improved GA and conventional GA.

Results	Improved GA	Conventional GA	Difference
TAP	1.0024	1.0025	0.01%
Q^{SC}	0.4612MVAr	0.4619MVAr	0.01%
P^{WT}	3.6315 MW	3.6312 MW	0.02%
Q^{WT}	1.2735MVAr	1.2732MVAr	0.02%
ΔU_{ave}	0.0366p.u.	0.0367p.u.	0.2%
ΔP_{loss}	1.6137 MW	1.6134 MW	0.01%
SATHD	0.23965%	0.23961%	0.02%
F(*x*)	0.62954	0.62942	0.01%
Calculation Time	120.266 s	302.134 s	181.868s

3.2. *Testing using the IEEE 33-bus system*

In this Subsection, a modified IEEE 33-bus system [29,43] shown in Fig. 4, is used to test feasibility of the proposed improved GA and to provide hourly optimization results, also demonstrating application of the two different *Q-control strategies* based on (18) and (19) respectively. Here the system modification is referred to the inclusion of WT and shunt capacitors. As a note, in the proposed ORPD strategy, distribution system power flows are used for obtaining electrical quantities necessary for objective function.

3.2.1. *Comparison between improved GA and conventional GA*

Accuracy and convergence of the proposed improved GA are compared with accuracy and convergence of the traditional GA. In Fig. 5 the convergence characteristic curves for both conventional and improved GA are given. *Setting 1* is used for weighting coefficients (see Section 3.1). As a heuristic search algorithm, GA may have different contingency route in each run. Therefore, randomly selected 5 curves out of 100 different tests, in which the population size, N_P, was 50, are presented in Fig. 4 to demonstrate the improved GA family of curves. The forecasted WT output active power limit and the load demand are both assumed to be 1p.u. The WT reactive output power limit was calculated according to the *Q-control strategy 2*.

As can be seen in Fig. 5, the proposed improved strategy:

i) always converges to the same optimal point for which adaptive value of objective function equals to 0.62954,
ii) always converges in less than 15 generations.

Under the same situation, the conventional GA requires much more generations to achieve the optimal point. When considering hourly modifications in real networks with higher complexity and more control variables, it is critical important to minimize calculation time in order to

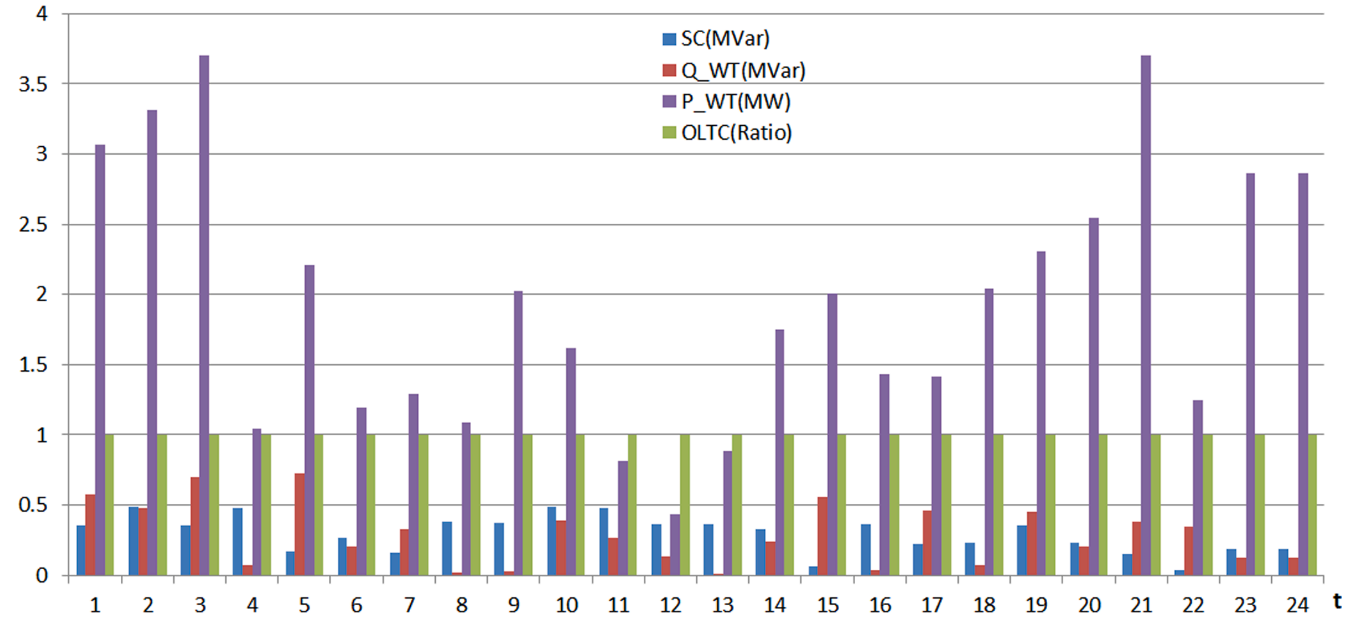

Fig. 7. Results of ORPD obtained with *Q-control strategy 1* for IEEE 33 bus system with WT.

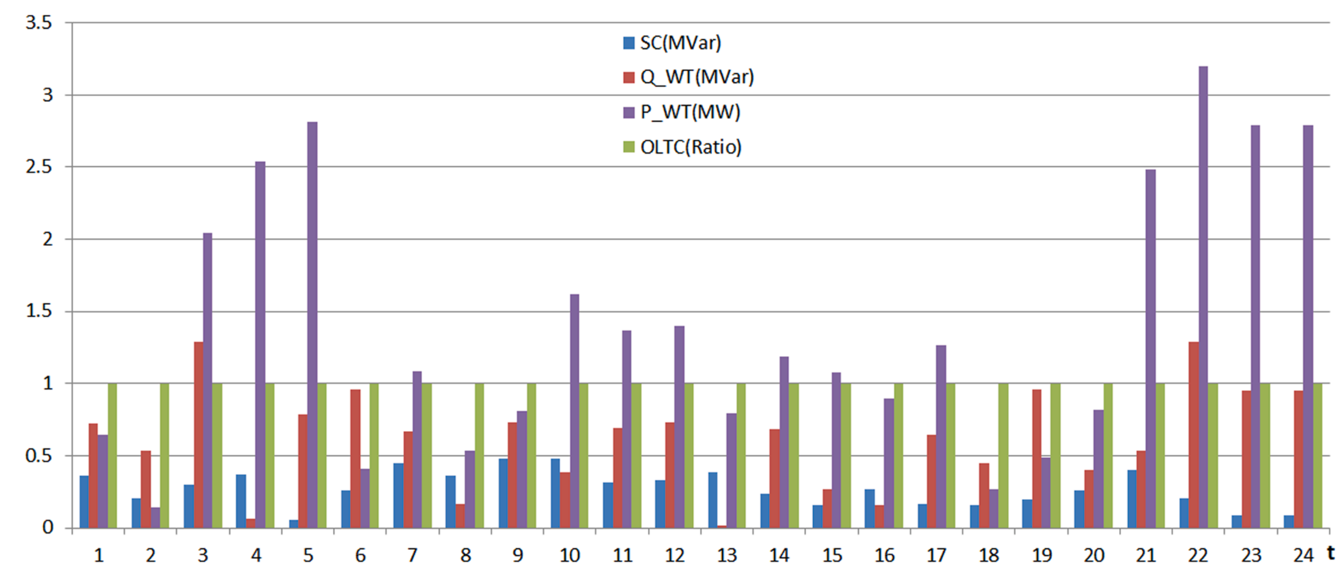

Fig. 8. Results of ORPD obtained with *Q-control strategy 2* for IEEE 33 bus system with WT.

against forecast errors. So the improvements of the proposed solver are essentially necessary compared with conventional GA. In Table 2 the outputs obtained by both improved and conventional GA are shown. All settings are within the system limits. As can be seen, the differences in results obtained by both algorithms are very small. It can be concluded that for a faster speed the accuracy has not been compromised.

3.2.2. Optimization results of each hour

Optimization results of each hour for the IEEE 33-bus test system are provided under two different *Q-control strategies* based on (18) and (19) respectively. A typical load demand curve and WT active power prediction curve [45] are used in this simulation. The predicted inputs of each hour, used in this study, are shown in Fig. 6.

As for the hourly modifications, considering the worst situation, the forecast errors are simulated in the case when load demand increases to the upper limit and WT output decreases to the lower limit which are ± 10% respectively. So it is assumed hourly modifications have been performed for every hour.

Based on these inputs for both time scales, two *Q-control strategies* with different reactive power limits of DFIG are simulated. Weighting coefficients defined through *setting 1* (see Section 3.1) are used.

The *Q-control strategy 1* defines the output reactive power limits using (18). By this, the 24 h histogram of calculated results is shown in Fig. 7. The *Q-control strategy 2* uses DFIG's maximum output reactive power capability that can be extended based on (19). The calculation results histogram for *Q-control strategy 2* is shown in Fig. 8.

From the results obtained, it can be concluded that:

i) output results for all control variables and each of four criteria are within power system constraints;
ii) comparing WT reactive power outputs in Fig. 7 and Fig. 8, it can be seen that more reactive power compensation will be made by WT when *Q-control strategy 2* is applied to DFIG;

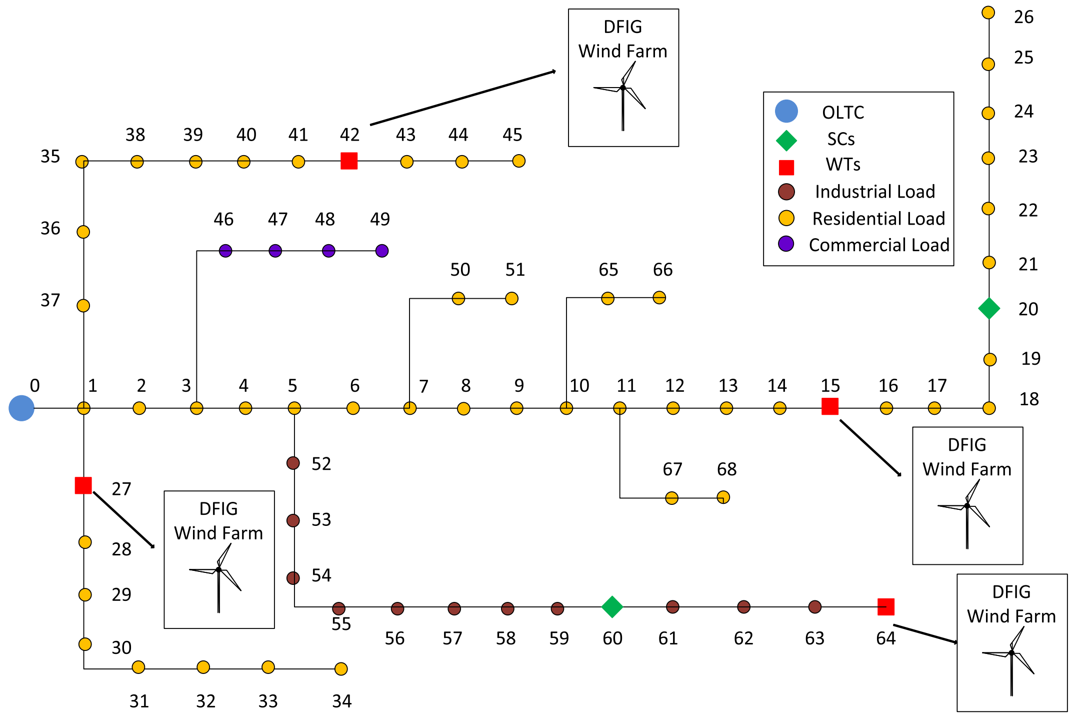

Fig. 9. Topology of modified PG&E 69-bus distribution system.

Table 3
Optimization results for PG&E 69-bus system with different weighting coefficients settings.

Scenarios	$F(x)$	ΔP_{loss} (%)	ΔU_{ave} (p.u.)	N_{TAP}	$SATHD$ (%)
Setting 1	0.5776	2.62	0.06263	0	1.79
Setting 2	0.5829	2.63	0.06143	0.0005	1.81
Setting 3	0.5674	2.62	0.06076	0	3.42
Results [29]	NA	2.82	0.08880	0	NA

Table 4
Optimization results for PG&E 69-bus system at different times of a day.

t		$F(x)$	ΔP_{loss} (%)	ΔU_{ave} (p.u.)	OLTC Ratio	SA THD (%)	Calculation Time (s)
1^{00}	DA	0.5719	2.62	0.06147	1.0005	1.78	180.622
	HM	0.5776	2.62	0.06263	1.0005	1.79	180.262
5^{00}	DA	0.5948	2.40	0.07405	1.0005	1.50	184.673
	HM	0.6029	2.40	0.07843	1.0005	1.59	180.416
9^{00}	DA	0.5274	1.52	0.06253	1.0004	1.07	194.524
	HM	0.5287	1.58	0.06976	1.0004	1.09	189.360
13^{00}	DA	0.5264	1.30	0.07735	1.0004	0.81	190.860
	HM	0.5293	1.35	0.07919	1.0004	0.76	184.539
17^{00}	DA	0.5045	1.22	0.06318	1.0004	0.95	192.797
	HM	0.5060	1.27	0.06358	1.0004	0.94	189.157
21^{00}	DA	0.6136	2.01	0.08236	1.0004	1.81	192.906
	HM	0.6487	2.05	0.08548	1.0004	1.82	184.773

iii) for both *Q-control strategies*, the optimization results of WT output active power are changing similarly to typical wind power prediction curve shown in Fig. 6. For instance, at night, the forecasted WT output active power capability is higher and, in the optimization results, the WT output active power is relatively high.

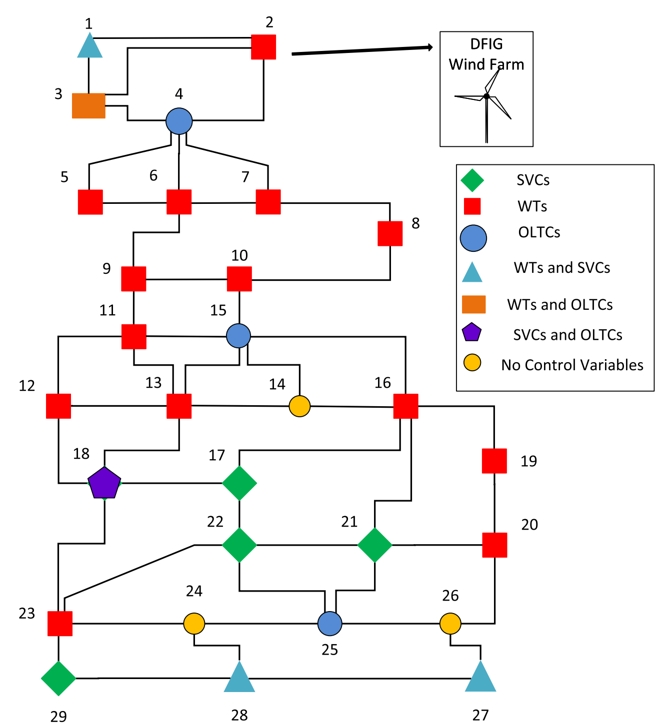

Fig. 10. Topology of the modified GB network.

Hence, the proposed ORPD strategy has made full use of the renewable energy resources and has provided reasonable results for each hour considering system operation nature.

3.3. Testing using PG&E 69-bus system

To test the proposed strategy on more complex test system with more control variables required, a modified PG&E 69-bus system has been

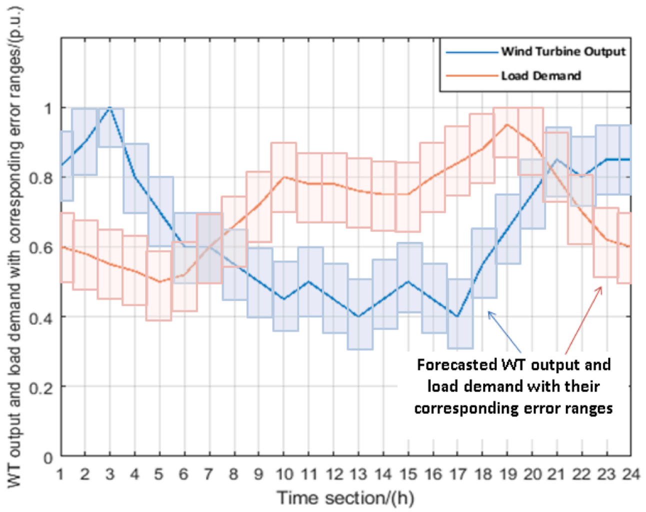

Fig. 11. Forecasted WT output and load demand with their corresponding error ranges.

used in this Subsection. Firstly, weighting coefficients are varied to analyse the sensitivity of four criteria and objective function to changes in importance of each criterion. In addition, each hour optimization is performed using typical load demand and WT active power prediction curves (Fig. 6), followed by hourly modifications. The topology of modified PG&E 69-bus system is shown in Fig. 9. Four DFIGs connected to the test system are assumed to be controlled by *Q-control strategy 2*.

3.3.1. Sensitivity study to the selection of weighting coefficients

To test the sensitivity of each criterion in the proposed ORPD strategy, different settings of weighting coefficients have been simulated separately (see Section 3.1). Data at 1AM are used for comparison between different scenarios. Additionally, the test results have been compared with results provided in [29]. All the results are summarized in Table 3.

In case of the proposed ORPD strategy (first three rows), it can be seen that the optimal results for the multi-objective function are similar for different scenarios. However, with different settings of weighting coefficients, each single criterion has different optimization result. With higher weighting coefficient, the criterion will be further optimized. In real system, this setting should be selected based on the system operation priority. In this paper, *setting 1* of weighting coefficients is chosen to do later simulations. The optimization strategy given in [29] considers only two criteria which are power losses and voltage deviation. When comparing the ORPD strategy with the one given in [29], the proposed strategy achieves better results for both criteria. This shows the priority of the new strategy.

3.3.2. Optimization results of each hour

For each hour optimization, both day-ahead and hourly modifications have been simulated. The results are shown for every four hours in Table 4. From the simulation results, the calculation time is within 4 mins for each hour, which is faster than reference [7] that also uses GA based approach for solving their objective function. For day-ahead optimization, typical load demand and WT active power prediction curves are used. For hourly modifications, considering the worst situation, they are simulated in the case when load demand increases to the upper limit and WT output decreases to the lower limit. Under this situation, the proposed strategy can still achieve hourly modifications with optimal results for all criteria by finishing calculations within 4 min. This shows the feasibility to apply the proposed ORPD strategy into real systems.

3.4. Testing using the GB network

Both IEEE 33 and PG&E 69 bus systems are distributions networks. To demonstrate the feasibility of the proposed ORPD strategy at the transmission level, the modified GB network with extensive involvement

Table 5
Optimization results for GB modified network at three different times of a day.

t	RESULTS	TRADITIONAL OPF		PROPOSED ORPD STRATEGY	
		Day Ahead	Hourly Modifications	Day Ahead	Hourly Modifications
1^{00}	$F(x)$	0.1823	0.1845	0.15724	0.15749
	P^{WT} (MW)	16708.03	15961.31	11167.27	9914.72
	Q^{WT} (MVAr)	171.2	160.3	4564.8	4426.5
	Q^{SC} (MVAr)	25.182	38.548	51.612	80.911
	ΔP_{loss} (%)	1.82	1.82	1.25	1.26
	ΔU_{ave} (p.u.)	0.01702	0.018031	0.015281	0.016653
	N_{TAP}	0.004	NA	0.002	NA
	$SATHD$ (%)	1.15	1.14	0.66	0.64
13^{00}	$F(x)$	0.15602	0.15611	0.14267	0.14301
	P^{WT} (MW)	14432.89	11383.60	9773.78	9517.53
	Q^{WT} (MVAr)	143.2	90.8	2798.5	2341.6
	Q^{SC} (MVAr)	35.9557	884.2694	101.112	580.5849
	ΔP_{loss} (%)	1.54	1.53	1.25	1.28
	ΔU_{ave} (p.u.)	0.016167	0.017291	0.016084	0.016846
	N_{TAP}	0.002	NA	0.001	NA
	$SATHD$ (%)	0.78	0.74	0.45	0.43
19^{00}	$F(x)$	0.17110	0.17238	0.15141	0.15176
	P^{WT} (MW)	21655.87	19394.24	14153.34	14117.50
	Q^{WT} (MVAr)	219.3	138.9	5312.2	4870
	Q^{SC} (MVAr)	1080.255	1233.2497	1081.629	1297.7268
	ΔP_{loss} (%)	1.55	1.53	1.17	1.15
	ΔU_{ave} (p.u.)	0.014364	0.014909	0.013127	0.013344
	N_{TAP}	0.004	NA	0.002	NA
	$SATHD$ (%)	0.84	0.80	0.58	0.57

of control devices is used. The topology of the modified GB transmission network is shown in Fig. 10 [46]. This network consists of 29 buses, 99 transmission lines and 65 generators. Core control devices in this system are 5 OLTCs, 18 WTs with DFIGs and 8 SVCs. HVDC links are not considered as control devices owing to their time-consuming operation scheme. The power flow for this test network is calculated using MATPOWER. The traditional OPF calculation results are used for comparison to express the merits of the proposed ORPD strategy.

Based on data from National Grid ESO website [47], WT output and load demand hourly forecast with the estimated forecast errors have been shown in Fig. 11.

Based on the forecasted data and the corresponding error ranges, the optimized reactive power dispatch strategy has been simulated and compared with the traditional OPF strategy. To consider the worst operation conditions, WTs output active power limit is set as the minimum value of the error range and the load demand is set as the maximum value of the error range. As for weighting coefficients, *setting1* is used and WTs are with *Q-control strategy 2* constraints. Simulation results for three randomly selected hours have been shown in Table 5.

The traditional OPF results are obtained using existing GB network optimization strategy with only active power cost as the objective function. Comparing the traditional OPF simulation results and the proposed ORPD strategy simulation results for three different hours of a day, it can be clearly concluded that all criteria can be effectively optimized via proposed ORPD strategy. This means by implementing the proposed ORPD strategy, GB network will be operated in a more stable and secure manner. Additionally, calculation time for all hourly modification simulation cases is within 3 min. This means after using the day-ahead forecast data to set the initial settings for the involved control devices, hourly modifications based on real-time data can still be calculated within 3 min even the worst forecast errors happened.

4. Conclusion

In this paper a new optimized reactive power dispatch (ORPD) strategy is proposed and successfully applied to optimize the operation of power systems with integrated wind power generation, at both distribution and transmission levels. This is achieved by solving the objective function using heuristic search algorithm to avoid approximation errors caused by analysis methods applied into large transmission networks. Compared with the existing strategies, (i) a more comprehensive objective function is proposed to achieve multi-objective optimization simultaneously, (ii) more control variables are considered and (iii) an improved GA based heuristic search algorithm for solving the proposed objective function is used. The core of the strategy is adequately formulated constrained mixed integer multi-objective problem, considering (a) system losses, (b) voltage deviations, (c) OLTCs and (d) system harmonic distortions. Additionally, as shown through the strategy testing, the proposed improved genetic algorithm combining i-NSGA-II and roulette selection for solving the optimization problem significantly increases the convergence speed without compromising the algorithm accuracy. This is particularly important for efficient and timely hourly modifications of control variables, i.e. wind generators' and reactive power compensators' power injections, as well as positions of taps at OLTCs. The importance of the hourly modifications is also demonstrated. This modification process resolves the uncertainties resulting from the discrepancy between forecasted and real-time measured data. Next to results describing different features of the new strategy, e.g. superior performances compared to previously published approaches, a general conclusion is that the algorithm can be applied in real control centres.

Declaration of Competing Interest

The authors declare that they have no known competing financial interests or personal relationships that could have appeared to influence the work reported in this paper.

Acknowledgement

Work of Y.Liu, D.Cetenovic and H.Li was supported by The University of Manchester and National Grid, UK, project number NGTO043 (R124809). Work of E.Gryazina and V.Terzija was supported by Skoltech and The Ministry of Education and Science of Russian Federation, Grant Agreement No 075-10-2021-067, Grant identification code 000000S707521QJX0002.

References

[1] Sun H, et al. Review of Challenges and Research Opportunities for Voltage Control in Smart Grids. IEEE Trans Power Syst July 2019;34(4):2790–801.
[2] Bansilal D. Thukaram, K. Parthasarathy, “Optimal reactive power dispatch algorithm for voltage stability improvement,” in International Journal of Electrical Power & Energy Systems, Volume 18, Issue 7, 1996, Pages 461-468, ISSN 0142-0615.
[3] Zhang W, Li F, Tolbert LM. Review of Reactive Power Planning: Objectives, Constraints, and Algorithms. IEEE Trans Power Syst Nov. 2007;22(4):2177–86.
[4] Kaloudas CG, Ochoa LF, Marshall B, Majithia S, Fletcher I. Assessing the Future Trends of Reactive Power Demand of Distribution Networks. IEEE Trans Power Syst Nov. 2017;32(6):4278–88.
[5] Liaoyi Ning, Wenchuan Wu, Boming Zhang, Pei Zhang, “A time-varying transformer outage model for on-line operational risk assessment,” in International Journal of Electrical Power & Energy Systems, Volume 33, Issue 3, 2011, Pages 600-607, ISSN 0142-0615.
[6] Alireza Hoseinpour, S. Masoud Barakati, Reza Ghazi, “Harmonic reduction in wind turbine generators using a Shunt Active Filter based on the proposed modulation technique,” International Journal of Electrical Power & Energy Systems, Volume 43, Issue 1, 2012, Pages 1401-1412, ISSN 0142-0615.
[7] Chen L, Li H. Optimized Reactive Power Supports Using Transformer Tap Stagger in Distribution Networks. IEEE Trans Smart Grid July 2017;8(4):1987–96.
[8] Yang Z, Bose A, Zhong H, Zhang N, Xia Q, Kang C. Optimal Reactive Power Dispatch With Accurately Modeled Discrete Control Devices: A Successive Linear Approximation Approach. IEEE Trans Power Syst May 2017;32(3):2435–44.
[9] “Wind Turbine Generator Systems, Part 21: Measurement and Assessment of Power Quality Characteristics of Grid Connected Wind Turbines”, IEC 61400-21, 2008.
[10] Liu J, Chen Y, Duan C, Lin J, Lyu J. Distributionally Robust Optimal Reactive Power Dispatch with Wasserstein Distance in Active Distribution Network. J Mod Power Syst Clean Energy May 2020;8(3):426–36.
[11] Gao H, Liu J, Wang L. Robust Coordinated Optimization of Active and Reactive Power in Active Distribution Systems. IEEE Trans Smart Grid Sept. 2018;9(5):4436–47.
[12] Ding T, Liu S, Yuan W, Bie Z, Zeng B. A Two-Stage Robust Reactive Power Optimization Considering Uncertain Wind Power Integration in Active Distribution Networks. IEEE Trans Sustainable Energy Jan. 2016;7(1):301–11.
[13] López J, Pozo D, Contreras J, Mantovani JRS. A Multiobjective Minimax Regret Robust VAr Planning Model. IEEE Trans Power Syst May 2017;32(3):1761–71.
[14] Ding T, Yang Q, Yang Y, Li C, Bie Z, Blaabjerg F. A Data-Driven Stochastic Reactive Power Optimization Considering Uncertainties in Active Distribution Networks and Decomposition Method. IEEE Trans Smart Grid Sept. 2018;9(5):4994–5004.
[15] Xu X, Yan Z, Shahidehpour M, Li Z, Yan M, Kong X. Data-Driven Risk-Averse Two-Stage Optimal Stochastic Scheduling of Energy and Reserve With Correlated Wind Power. IEEE Trans Sustainable Energy Jan. 2020;11(1):436–47.
[16] Ahmet Öner, Ali Abur, “Computationally efficient method for placing reactive power sources against contingencies,” in International Journal of Electrical Power & Energy Systems, Volume 133, 2021, 107253, ISSN 0142-0615.
[17] Xi Zeng, Hongbin Wu, Ming Ding, Rui Bi, Bin Xu, Jinjin Ding, “Two-stage robust optimization for practical reactive power in distribution network based on multiple constraint convex approximation,” in International Journal of Electrical Power & Energy Systems, Volume 134, 2022, 107414, ISSN 0142-0615.
[18] Garcia M, Baldick R. Approximating Economic Dispatch by Linearizing Transmission Losses. IEEE Trans Power Syst March 2020;35(2):1009–22.
[19] Low SH. Convex Relaxation of Optimal Power Flow—Part I: Formulations and Equivalence. IEEE Trans Control Network Syst March 2014;1(1):15–27.
[20] Juan M. Ramirez, Juan M. Gonzalez, Tapia O. Ruben, “An investigation about the impact of the optimal reactive power dispatch solved by DE,” in International Journal of Electrical Power & Energy Systems, Volume 33, Issue 2, 2011, Pages 236-244, ISSN 0142-0615.
[21] T. Malakar, Abhishek Rajan, K. Jeevan, Pinaki Dhar, “A day ahead price sensitive reactive power dispatch with minimum control,” in International Journal of Electrical Power & Energy Systems, Volume 81, 2016, Pages 427-443, ISSN 0142-0615.
[22] Shaheen AM, Elsayed AM, Ginidi AR, Elattar EE, El-Sehiemy RA. Effective Automation of Distribution Systems With Joint Integration of DGs/ SVCs Considering Reconfiguration Capability by Jellyfish Search Algorithm. IEEE Access 2021;9:92053–69.

[23] Khan NH, Wang Y, Tian D, Jamal R, Kamel S, Ebeed M. Optimal Siting and Sizing of SSSC Using Modified Salp Swarm Algorithm Considering Optimal Reactive Power Dispatch Problem. IEEE Access 2021;9:49249–66.

[24] Elsayed SK, Kamel S, Selim A, Ahmed M. An Improved Heap-Based Optimizer for Optimal Reactive Power Dispatch. IEEE Access 2021;9:58319–36.

[25] Barun Mandal, Provas Kumar Roy, "Optimal reactive power dispatch using quasi-oppositional teaching learning based optimization," in International Journal of Electrical Power & Energy Systems, Volume 53, 2013, Pages 123-134, ISSN 0142-0615.

[26] Ruey-Hsun Liang, Jia-Ching Wang, Yie-Tone Chen, Wan-Tsun Tseng, "An enhanced firefly algorithm to multi-objective optimal active/reactive power dispatch with uncertainties consideration," in International Journal of Electrical Power & Energy Systems, Volume 64, 2015, Pages 1088-1097, ISSN 0142-0615.

[27] Susanta Dutta, Pranabesh Mukhopadhyay, Provas Kumar Roy, Debashis Nandi, "Unified power flow controller based reactive power dispatch using oppositional krill herd algorithm," in International Journal of Electrical Power & Energy Systems, Volume 80, 2016, Pages 10-25, ISSN 0142-0615.

[28] Mehdi Mehdinejad, Behnam Mohammadi-Ivatloo, Reza Dadashzadeh-Bonab, Kazem Zare, "Solution of optimal reactive power dispatch of power systems using hybrid particle swarm optimization and imperialist competitive algorithms," in International Journal of Electrical Power & Energy Systems, Volume 83, 2016, Pages 104-116, ISSN 0142-0615.

[29] Chen L, Deng Z, Xu X. Two-Stage Dynamic Reactive Power Dispatch Strategy in Distribution Network Considering the Reactive Power Regulation of Distributed Generations. IEEE Trans Power Syst March 2019;34(2):1021–32.

[30] S. Jeyadevi, S. Baskar, C.K. Babulal, M. Willjuice Iruthayarajan, "Solving multiobjective optimal reactive power dispatch using modified NSGA-II," in International Journal of Electrical Power & Energy Systems, Volume 33, Issue 2, 2011, Pages 219-228, ISSN 0142-0615.

[31] Hong Y-Y, Ho S-Y. Determination of network configuration considering multiobjective in distribution systems using genetic algorithms. IEEE Trans Power Syst May 2005;20(2):1062–9.

[32] Zhang M, Li Y. Multi-Objective Optimal Reactive Power Dispatch of Power Systems by Combining Classification-Based Multi-Objective Evolutionary Algorithm and Integrated Decision Making. IEEE Access 2020;8:38198–209.

[33] Xiong H, Cheng H, Li H. Optimal reactive power flow incorporating static voltage stability based on multi-objective adaptive immune algorithm. Energy Coversion and Management May 2008;49:1175–81.

[34] Kumar M, Guria C. The elitist non-dominated sorting genetic algorithm with inheritance (i-NSGA-II) and its jumping gene adaptations for multi-objective optimization. Information Sciences, Volumes 2017;382–383:15–37.

[35] Da Silva EL, Gil HA, Areiza JM. Transmission network expansion planning under an improved genetic algorithm. IEEE Trans Power Syst Aug. 2000;15(3):1168–74.

[36] Saša Vlahinić, Dalibor Brnobić, Dubravko Vučetić, "Measurement and analysis of harmonic distortion in power distribution systems," in Electric Power Systems Research, Volume 79, Issue 7, 2009, Pages 1121-1126, ISSN 0378-7796.

[37] F. Sayadi, S. Esmaeili and F. Keynia, "Two-layer volt/var/total harmonic distortion control in distribution network based on PVs output and load forecast errors," in IET Generation, Transmission & Distribution, vol. 11, no. 8, pp. 2130-2137, 1 6 2017.

[38] Abbas Ketabi, Mohammad Reza Sheibani, Seyyed Mostafa Nosratabadi, "Power quality meters placement using seeker optimization algorithm for harmonic state estimation," in International Journal of Electrical Power & Energy Systems, Volume 43, Issue 1, 2012, Pages 141-149, ISSN 0142-0615.

[39] Niancheng Zhou, Fangqing Sun, Qianggang Wang, Xiaoxiao Meng, "A flexible power control strategy for rotor-side converter of DFIG under unbalanced grid voltage sags," in International Journal of Electrical Power & Energy Systems, Volume 90, 2017, Pages 64-75, ISSN 0142-0615.

[40] Lasantha Meegahapola, Sarath Perera, "Capability constraints to mitigate voltage fluctuations from DFIG wind farms when delivering ancillary services to the network," in International Journal of Electrical Power & Energy Systems, Volume 62, 2014, Pages 152-162, ISSN 0142-0615.

[41] Ghosh S, Isbeih YJ, Bhattarai R, Moursi MSE, El-Saadany EF, Kamalasadan S. A Dynamic Coordination Control Architecture for Reactive Power Capability Enhancement of the DFIG-Based Wind Power Generation. IEEE Trans Power Syst July 2020;35(4):3051–64.

[42] Deb K, Pratap A, Agarwal S, Meyarivan T. A fast and elitist multi objective genetic algorithm: NSGA-II. IEEE Trans Evol Comput April 2002;6(2):182–97.

[43] Zhang P, Li W, Wang S. Reliability-oriented distribution network reconfiguration considering uncertain-ties of data by interval analysis. Int J Electr Power Energy Syst 2012;34:138–44.

[44] Chengfu Wang, Xijuan Li, Zhaoqing Wang, Xiaoming Dong, Zhengtang Liang, Xiaoyi Liu, Jun Liang, Xueshan Han, "Day-ahead unit commitment method considering time sequence feature of wind power forecast error," in International Journal of Electrical Power & Energy Systems, Volume 98, 2018, Pages 156-166, ISSN 0142-0615.

[45] Bludszuweit H, Dominguez-Navarro JA, Llombart A. Statistical analysis of wind power forecast error. IEEE Trans Power Syst Aug. 2008;23(3):983–91.

[46] L. P. Kunjumuhammed, B. C. Pal and N. F. Thornhill, "A test system model for stability studies of UK power grid," 2013 IEEE Grenoble Conference, Grenoble, 2013, pp. 1-6.

[47] Extranet.nationalgrid.com. 2020. BSAD. [online] Available at: <https://extranet.nationalgrid.com/BSAD/> [Accessed 19 December 2020].